Smart Health 16 (2020) 100106

Contents lists available at ScienceDirect

Smart Health

journal homepage: www.elsevier.com/locate/smhl

Development and feasibility test of a capacitive belt sensor for noninvasive respiration monitoring in different postures

Dae Gyeom Kim [a], Changwon Wang [a], Jong Gab Ho [a], Se Dong Min [a], Young Kim [c,*], Min-Hyung Choi [b]

[a] Department of Medical IT Engineering, Soonchunhyang University, Asan, 31538, South Korea
[b] Department of Computer Science and Engineering, University of Colorado Denver, Denver, CO, 80217-3364, USA
[c] Wellness Coaching Service Research Center, Soonchunhyang University, Asan, 31538, South Korea

ARTICLE INFO

Keywords:
Capacitive
Wearable
Belt sensor
Noninvasive
Respiration
Posture

ABSTRACT

The purpose of this study was to develop an easy-wear capacitive belt sensor, examine its performance, and test the feasibility for differentiating posture-dependent respiration changes, consequently for monitoring of variable respiration patterns during real life activities.

Seven healthy adult males participated in this study. Respiration (at rest) data were collected simultaneously from capacitive belt sensor and commercial sensor (BIOPAC MP150) for 3 min in each of the 6 different static postures representative of real-life activity postures: supine with neutral head position, standing, sitting, side lying, supine with 45° cervical flexion, and supine with 45° cervical extension.

From the collected data, 3 respiratory parameters including total respiration count (RC), peak to peak interval time (PPI), and respiratory rate (RR) were analyzed. Correlation analysis was conducted for all three of the parameters collected by the two sensors. The highest PPI values were found in cervical extension supine posture and the lowest in side lying. RC and PPI patterns were inversely related. The results of RR showed to have exactly the same pattern with RC; the highest rate was during standing and the lowest in cervical extension supine. The RRs detected by our sensor were within the normal range, confirming the performance and feasibility of our sensor.

As our sensor was able to detect posture-dependent respiration pattern differences, potential application in sleep apnea monitoring, respiratory disease prevention, and early detection of diagnostic symptoms has been confirmed.

1. Introduction

As healthcare and well-being are holding the limelight in the fourth industrial revolution era, developing light and efficient wearable sensors for continuous monitoring of various health conditions and attempts to find ways to detect diseases earlier, prevent obesity, and delay aging are gaining continuous attention from the medical and healthcare fields.

Respiratory activity being one of the vital signs is an important indicator of the basic health. Abnormalities in respiratory activity parameters can lead to medical emergencies (Guan et al., 2018). Monitoring of respiratory pattern has long been acknowledged as a significant identifier and a predictor of serious adverse events such as dyspnea, hypopnea, sleep apnea, and sudden death due to airway

* Corresponding author.
E-mail addresses: sedongmin@sch.ac.kr (S.D. Min), ykim02@sch.ac.kr (Y. Kim).

https://doi.org/10.1016/j.smhl.2020.100106

Available online 13 January 2020

obstruction, which are also closely related with aging and obesity (Al-Khalidi, Saatchi, Burke, Elphick, & Tan, 2011; Lee et al., 2018; Reyes, Reljin, Kong, Nam, & Chon, 2017).

Numerous studies have stated that tidal volume, minute ventilation, and respiratory rate are the basic markers for finding or predicting respiratory dysfunction (Houssein, Ge, Gastinger, Dumond, & Prioux, 2019; Schlesinger, 2015). Conventional and precise method to measure respiratory function is by using a spirometer, usually in a sitting posture, but its drawbacks are the need to wear a mouthpiece or a face mask, and a nose clip. Using optoelectronic plethysmography (OEP) to measure the changes in chest wall volume is another accurate method. Studies that applied OEP methods used at least 45 to 66 reflective markers to analyze respiration in supine, 81 markers for lateral position, and installed 6 to 8 infrared cameras to capture the movements (Nozoe et al., 2014). Despite the accuracy of OEP, the cumbersomeness of attaching and wearing dozens of markers for one experimental position can be the greatest disadvantage for both the researcher and the subject. To resolve these unpracticality, researchers have attempted developing alternatives to measure and estimate respiratory variables (Chhabra, 2015; Fekr, Radecka, & Zilic, 2015). One of our previous studies was also an attempt to develop a simple and comfortable capacitance-based textile respiration belt sensor. The study was successful in monitoring and analyzing the abdominal respiratory rate of healthy individuals in a sitting posture (Min, Yun, & Shin, 2014).

However, there is a need to consider that the human body has different postures at different times of the day and during different types of activities which in turn produce different respiratory activity. For this, we designed this study to develop an advanced respiration sensor and to test its performance in various daily-activity postures. As postures influence human respiratory activity, several studies tried detecting the changes in breathing patterns and mechanics in different postures (Aliverti et al., 2001; Cesareo, Previtali, Biffi, & Aliverti, 2018; Nozoe et al., 2014; Romei et al., 2010; Schellongowski et al., 2007; Sukul, Trefz, Kamysek, Schubert, & Miekisch, 2015).

A study by Nozoe et al. noted that their study was the first to show laterality of chest wall volume changes in lateral positions. They reported that changing postures from supine to lateral positions affect respiratory mechanics; it can change the amount of pulmonary gas exchange, ventilation to perfusion ratio, can cause expansion restrictions of the side contacting the floor, and increase the abdominal pressure (Nozoe et al., 2014; Schellongowski et al., 2007). However, these studies were conducted with the patients with cardiopulmonary, cardiovascular, cerebrovascular diseases, post-operation patients with pulmonary diseases, or in an intensive care unit setting and used OEP, inertial measurement unit (IMU), or other heavy and professional costly devices. Aliverti et al. studied the regional chest wall volume changes in the supine and prone positions in normal subjects (Aliverti et al., 2001), Romei et al. studied chest wall kinematics in sitting to supine positions and reported that chest wall volumes are affected by positions with gradually increasing contribution of the abdomen to tidal volume, and Cesareo et al. studied respiratory rate of healthy subjects in sitting and supine postures (Cesareo et al., 2018; Romei et al., 2010). However, none of these studies included lateral postures and static standing. A study by Sukul et al. included right and left side lying, sitting, standing, supine, and prone, but the results were only focused on compositions of exhaled breath (Sukul et al., 2015).

Current sensing methods are more focused on realizing no stress to the user. Among many wearable sensing techniques, soft sensors are known to be not restricting natural kinematics of human movement, but enabling long-term, comfortable monitoring of the wearer (Hughes & Iida, 2018). Soft strain sensors are promising for wearable applications since they are flexible, can be worn over clothes, and can determine pressure, oscillation, and displacement that occur during human movements (Hughes & Iida, 2018; Pegan et al., 2016). For this reason, this study chose to develop a flexible belt-type soft strain sensor to monitor respiration and differentiate the breathing patterns according to different postures.

Previous studies on wearable strain sensors for physiological measurement and monitoring were focused towards stretchable capacitive, percolating, and piezo-resistive sensor types (Pegan et al., 2016). Intelligent textiles such as knitted strain sensor or conductive thermoplastic fabric sensors developed in the form of a t-shirt or suites were also available. However, requiring the users to wear additional tight clothing for detection of strain changes was a disadvantage (Hughes & Iida, 2018). Among the mentioned, capacitive sensors were found to exhibit high sensitivity for detecting human movements from as subtle as pulsatile pressure to dynamic gross body movements and were considered applicable in various form factors (Li et al., 2016; Nie et al., 2010; Zens et al., 2015). In addition, previous studies have confirmed that measuring capacitance for respiration signal and the possibility of estimating air volume without straining the body were promising (Terazawa, Karita, Kumagai, & Sasaki, 2018).

Although belt-type sensors have been widely used for monitoring physical activity in clinical and lab-based settings, posture-specific respiration pattern monitoring studies considering the changes in body postures during daily activities have not been studied with a single capacitive belt sensor. Therefore in this study, an easy-wear belt-type capacitive sensor was developed and tested in comparison with a commercial sensor for detecting posture-specific respiration differences based on 6 representative postures in young healthy adults.

2. Method

2.1. Mechanism of capacitive belt sensor for respiration detection

To make an advanced version of our previous sensor, the newly developed capacitive belt sensor (CBS) in this study was designed with a 10-bit resolution, wireless, and compact capacitance measurement board capable of simultaneous collection of data from 10 channels. CBS detects the changes in the chest circumference based on the resistance force generated against the belt during inhalation and exhalation. This was based on parallel capacitance theory. Capacitance refers to the ability of an object to accumulate electric charge in the unit of Farad (F). 1 F is equal to the capacitance charged at 1 C (C) when 1 V (V) is applied to capacitor. Parallel capacitance can be calculated by the following equation (1).

$$C = \varepsilon \frac{A}{d} \tag{1}$$

where, ε is the permittivity material between the plates, d refers to the distance between two plates, and A refers to the area of plates.

Fig. 1 below shows the system architecture of our proposed sensor. CBS measured respiration signal and the printed circuit board (PCB) collected the respiration data at a sampling rate of 100 Hz using analog to digital converter (ADC). The collected data were then transferred to the monitoring application on a PC. Our monitoring application had a real-time display and saving functions. For signal processing, moving average filter, DC component removal, normalization, and peak detection by 'local maxima' extracting the respiration indices (respiration count (RC), peak to peak interval time (PPI), respiratory rate (RR)) were performed using Matlab2015a.

The CBS was developed using 5 layers of conductive textile as shown below in Fig. 2(a). It had a sensor layer, a ground layer, and three di-electric materials on the top, bottom, and in the center; separating the respiration sensor from the ground. The sensor and ground layers were developed using the TROS-10 model (Ajin Electronics, Busan, ROK), which is made up of polyolefin, nickel, and copper. The size of each layer was 3.5 cm × 2.5 cm. Fig. 2(b) shows the actual structure of CBS attached adjacent to our reference sensor BIOPAC MP150 RSP100C (BIOPAC Systems Inc., CA, USA).

The PCB was developed to collect capacitance values as illustrated in Fig. 2(c). For Micro Controller Unit (MCU), STM32F103 (STMicroelectronics, Geneva, Switzerland) was used. The MCU had 16 ADC channels, a 10-bit ADC resolution, and its driving voltage was 3.7 V. MPR121QR2 was used for converting analog to digital data. The MPR121QR2 (NXP, Eindhoven, Netherland) sensor has a

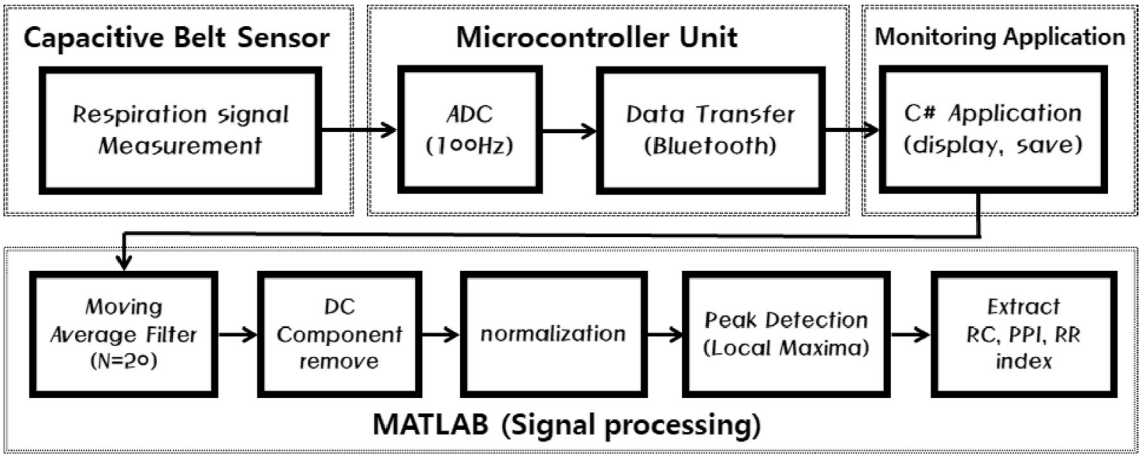

Fig. 1. System architecture.

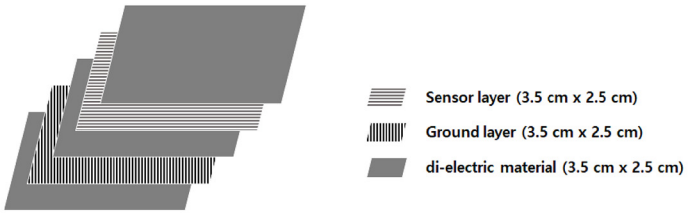

(a) The structure of capacitive belt sensor

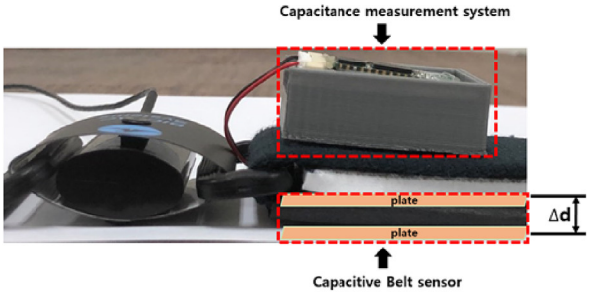

(b) Respiration signal detection system

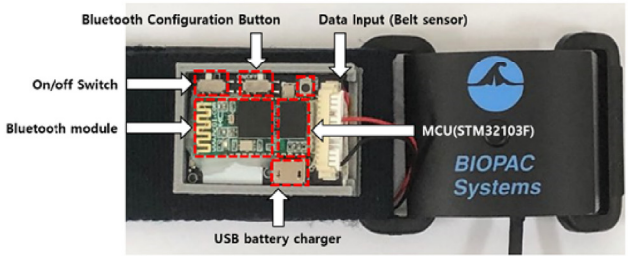

(c) Capacitance measurement board

Fig. 2. Structure of the developed capacitive belt sensor attached adjacent to MP150 (BIOPAC) sensor.

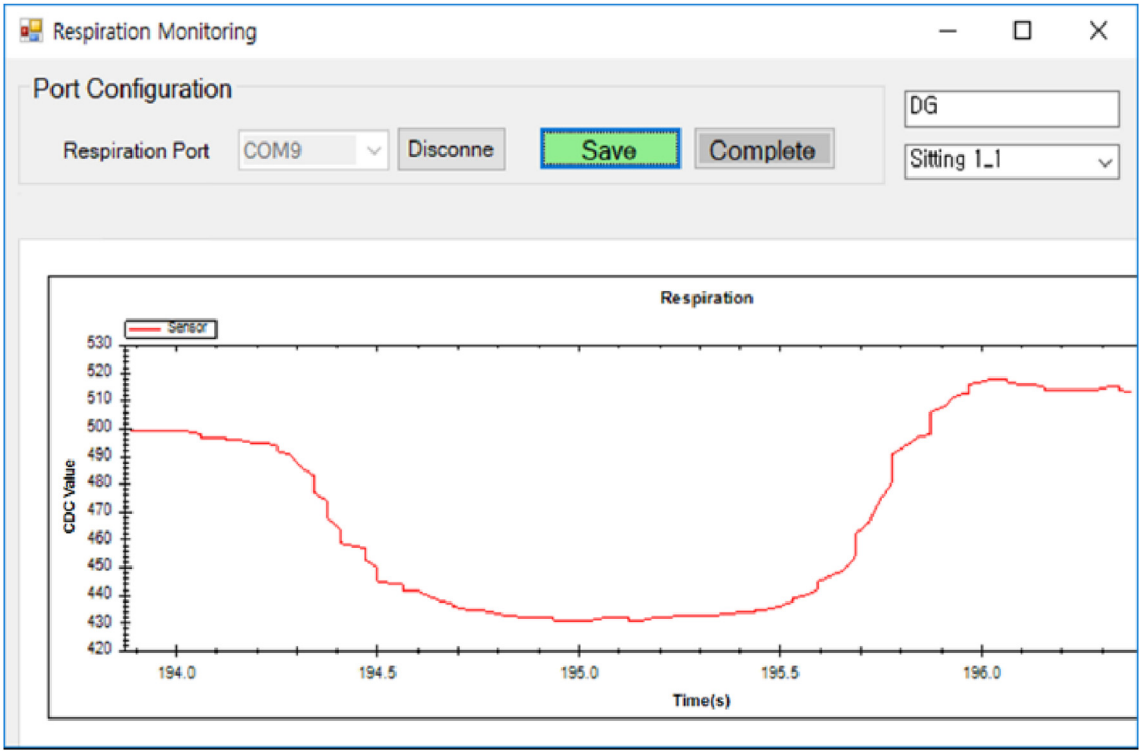

Fig. 3. The real-time display of respiration monitoring application.

resolution of capacitance between 0 and 2000 pico-Farad (pF). The capacitance data were sampled at 100 Hz and Bluetooth communication was used for transfer of data from PCB and PC monitoring application (baud-rate: 115200).

The monitoring application was developed using C# language as shown in Fig. 3. As shown, the application visualizes the real-time raw data of capacitance values changing accordingly with each subject's respiration in a graph (x-axis: time (second), y-axis: capacitance to digital converted value (CDC)) and the data can be saved in a text file including time stamp (yy-mm-dd-hh-mm-ss, yy: year, mm: month, dd: day, hh: hour, mm: minutes, ss: seconds).

2.2. Signal processing

To calculate respiration indicators, moving average filter (window size 20) and noise removal were performed for data smoothing using Matlab2015a as illustrated in Fig. 4. Local maxima algorithm was used for peak detection analysis after DC component removal and normalization. Total respiration count (RC), peak to peak interval time (PPI), respiratory rate (RR), and error rate were calculated based on peak point information.

Respiratory rate (RR) was calculated by equation (2) (Yang, Keller, Popescu, & Skubic, 2016).

$$\mathrm{RR} = \frac{60}{N} \sum_{n=1}^{N} \frac{1}{I(n)} \tag{2}$$

where, I(n) refers to each peak to peak interval time, N the total respiration count.

Error rate between CBS and MP150 was calculated by equation (3).

$$\text{Error rate}(\%) = \frac{|PPI_{CBS} - PPI_{REF}|}{PPI_{REF}} \times 100 \tag{3}$$

2.3. Placement of capacitive belt sensor

For detection and measurement of the respiratory parameters during respiration at rest, CBS was placed around the chest, on the fourth thoracic vertebra (T4) level as shown below in Fig. 5. CBS was located 2 cm laterally distanced from the xyphoid process, over the left pectoralis major (PM) muscle. MP150 sensor was placed over the right PM muscle; both of the two sensors were equally distanced from the midline, on the same T4 level. These two sensors were attached on a single elastic belt for simultaneous data collection and the tightness of the belt around T4 level was adjusted by the same researcher for conditional conformity of the experiment.

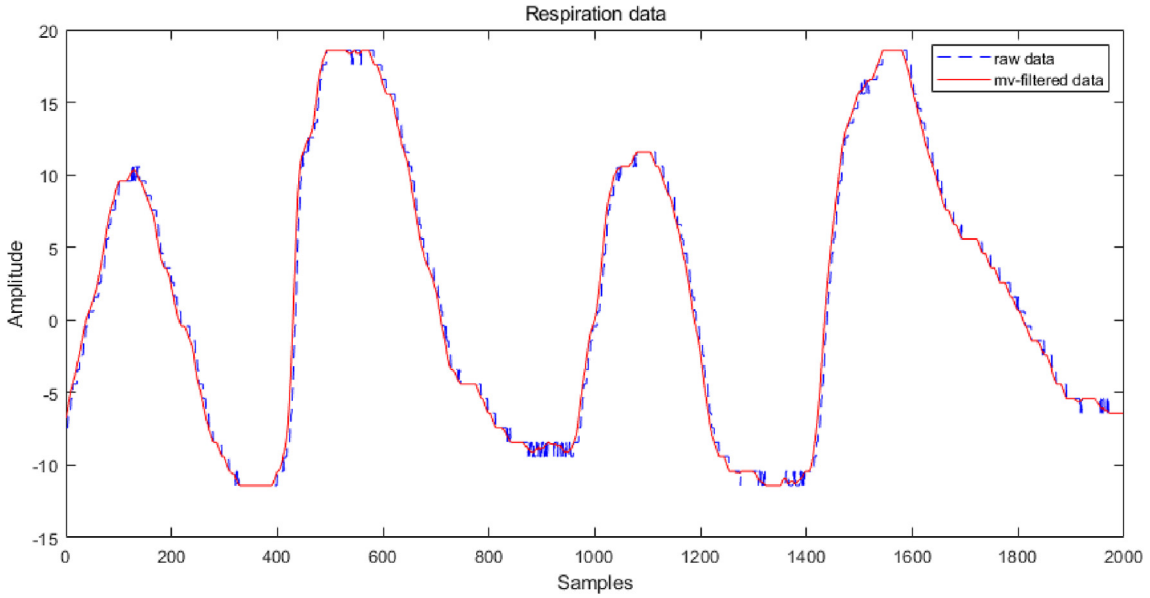

Fig. 4. Signal preprocessing sample image (moving average filter).

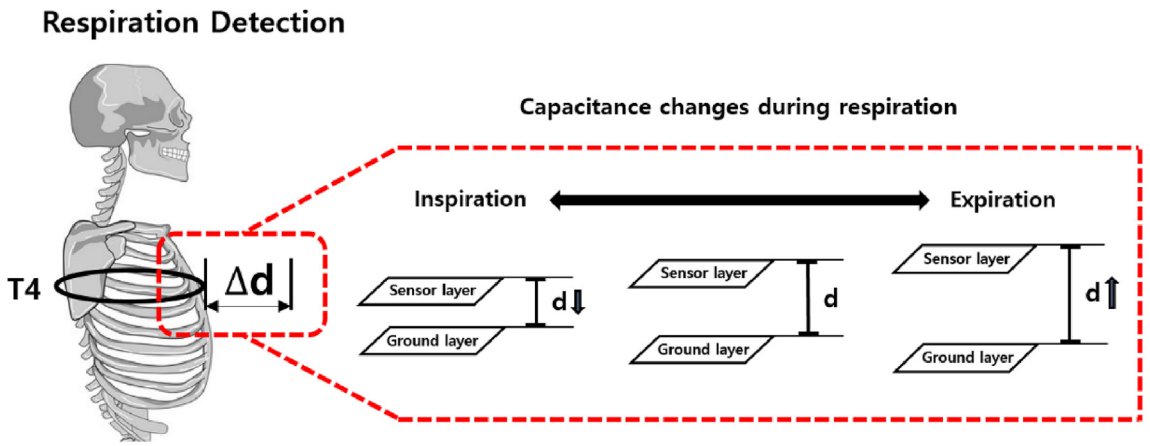

Fig. 5. Respiration detection by capacitive belt sensor on T4 level.

2.4. Experimental protocol

In this study, two-stage experiments were conducted. Experiment 1 (E1) was carried out for performance evaluation of CBS by examining the correlation between CBS and MP150 in different static postures for reliability and accuracy. Experiment 2 (E2) was performed to test the feasibility of CBS in differentiating posture-specific respirations. For the study, all subjects were asked to wear a given dry-fit elastic shirt for equal contact force of CBS as the movement of different type of clothes can cause interference in the capacitance output. Study purpose and procedures were adequately explained to the subjects and all participants signed the informed consent form.

2.4.1. Sensor performance evaluation (E1)

Seven healthy young male subjects participated in the experiment (mean age: 26.75 ± 2.71 yrs, height: 175.37 ± 6.02 cm, Weight: 72 ± 10.44 kg, BMI: 23.31 ± 2.21). General characteristics of the subjects are presented in Table 1. All subjects had no history of respiratory disorders, cardiopulmonary diseases, related surgeries or medications, and experience of ventilation difficulties during the past 6 months. For this study, respiration (at rest) data were collected simultaneously from CBS and MP150 for 3 min in 6 different static postures (refer to E2 below). From the collected data, 3 respiratory parameters (RC, PPI, and RR) were analyzed. Pearson's correlation analysis was conducted for all three of the parameters collected by the two sensors.

Table 1
Subject characteristics.

Subject No.	Gender	Age	Height (cm)	Weight (kg)	BMI (Body Mass Index)
Subject 1	male	23	182	82	24.75
Subject 2	male	27	178	66	20.83
Subject 3	male	26	168	66	23.38
Subject 4	male	32	182	89	26.86
Subject 5	male	28	175	77	25.14
Subject 6	male	27	168	62	21.96
Subject 7	male	24	170	59	20.41
AVG		26.75	175.37	72	23.31
SD		2.71	6.02	10.44	2.21

2.4.2. Sensor feasibility in differentiating posture-specific respirations (E2)

The same 7 subjects performed both E1 and E2 consecutively on the same day. For both E1 and E2, respiration data were collected in 6 different posture conditions, which are representative of real-life postures: supine with neutral head position (P1), standing (P2), sitting (P3), side lying (P4), supine with 45° cervical flexion (P5), supine with 45° cervical extension (P6). Postural conditions are illustrated in Fig. 6. For P1, P2, P3 postures, subjects' head was positioned into the cervical neutral position by a physical therapist. All subjects were then instructed to maintain the posture throughout the experiment. Verbal and tactile cues were provided by the therapist when needed. For P2 posture, subjects were instructed to place their feet apart in alignment with the width of their pelvis (distance between right and left anterior superior iliac spine (ASIS)). To help the subjects keep the same posture during the experiment, the space between the 1st metatarsal head of the both feet was measured and marked on the floor. For P3 posture, the knee and hip joint in 90° flexion was to be maintained with the trunk straight, against the back of the given chair. For P4 posture, a pillow was placed under the head and another one between the legs to keep the spine straight. For P5 and P6, two pillows were placed under the scapula to make cervical flexion and extension postures, respectively. Subjects' passive cervical range of motion was tested prior to study and the conditional postures (P5, P6) were positioned by the same physical therapist. Each of the 6 postures were maintained for 3 min with 1-min resting time in between the conditions. The order of postural conditions was randomly selected for each subject. The first and last 30 s of the collected data were deleted to remove start/stop effects and the mid 2 min of respiration was used for analysis (Guan et al., 2018; Min et al., 2014).

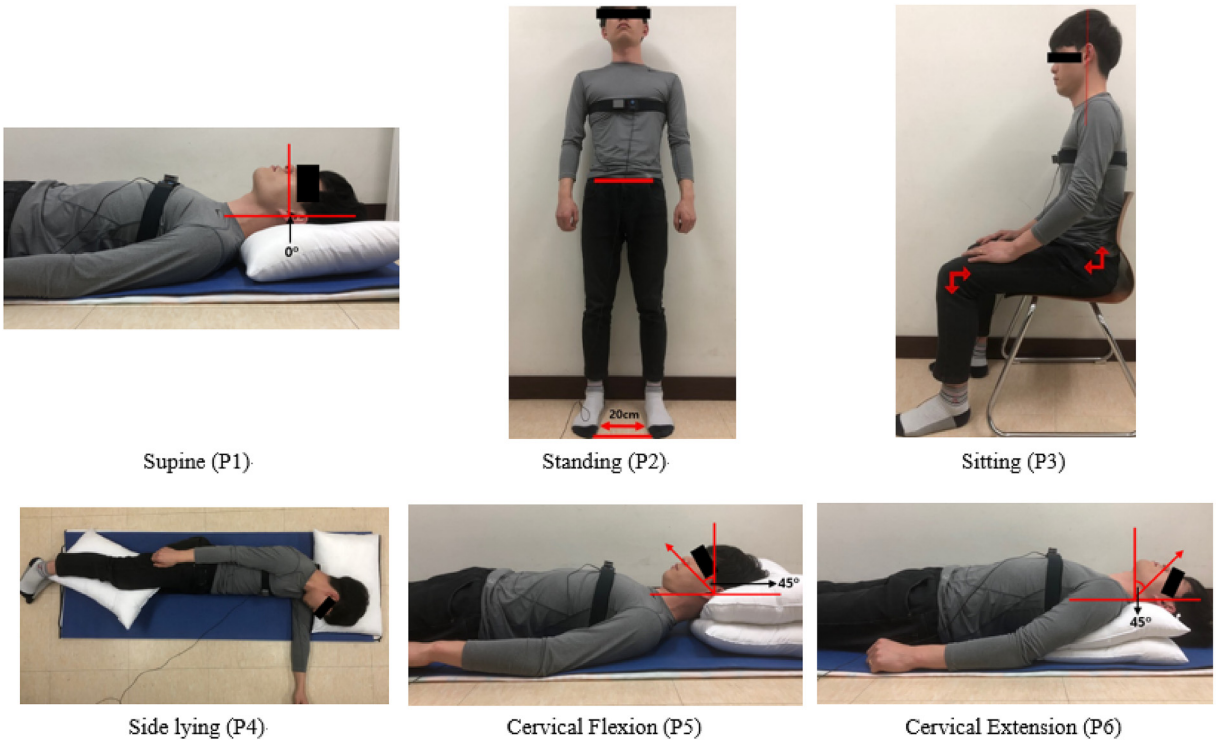

Fig. 6. Six experimental posture conditions (E2).

3. Results

3.1. Results of correlation analysis between CBS and MP150

3.1.1. Respiration count (RC)

Correlation of RC was found to be 100% consistent between CBS and MP150. Table 2 shows the numerical results of correlation analysis on RC detected by the two sensors for 2 min of breathing (Guan et al., 2018). The average RCs in each posture were 20.86 ± 7.49 (P1), 27.57 ± 8.98 (P2), 26.14 ± 10.62 (P3), 27 ± 6.93 (P4), 21.43 ± 5.71 (P5), and 18.71 ± 6.29 (P6). The highest RC was found in standing (P2) and the lowest in supine with cervical extension (P6), showing that standing caused hyperventilation compared to supine position with the neck extended.

3.1.2. Peak to peak interval time (PPI)

The results of average PPI time in 6 conditional postures with CBS were 6.33 ± 2.51 s (P1), 4.60 ± 1.42 s (P2), 5.07 ± 1.96 s (P3), 4.57 ± 1.05 s (P4), 5.79 ± 1.66 s (P5) and 6.91 ± 2.83 s (P6), respectively (Table 3). The highest PPI time was found in supine with cervical extension (P6) and the lowest in side-lying (P4), showing a slowed respiration in supine position with the neck extended. Average PPIs with MP150 in 6 postures were 6.33 ± 2.44 s (P1), 4.60 ± 1.42 s (P2), 5.06 ± 1.96 s (P3), 4.58 ± 1.06 s (P4), 5.76 ± 1.61 s (P5) and 6.90 ± 2.83 s (P6), respectively (Table 4). Highly similar results were found in both of the sensors. Bland-Altman plot showing the difference of PPI time in each posture in comparison between CBS and MP150 is in Fig. 7.

The results of Pearson's correlation analysis on PPI in each posture between CBS and MP150 are shown in Table 5 The average R^2 values in 6 postures were 0.91 ± 0.06 (P1), 0.90 ± 0.04 (P2), 0.90 ± 0.04 (P3), 0.92 ± 0.03 (P4), 0.91 ± 0.05 (P5), and 0.89 ± 0.03 (P6)

Table 2
Results of respiration count comparison between CBS and MP150 during 2-min breathing.

Subject No.	P1	P2	P3	P4	P5	P6	Consistency
Subject 1	21	23	25	36	21	16	100%
Subject 2	19	25	21	23	18	17	100%
Subject 3	24	28	27	26	25	22	100%
Subject 4	25	31	30	26	23	25	100%
Subject 5	13	16	14	22	19	9	100%
Subject 6	33	45	47	37	31	27	100%
Subject 7	11	25	19	19	13	15	100%
AVG	20.86	27.57	26.14	27	21.43	18.71	
SD	7.49	8.98	10.62	6.93	5.71	6.29	

P1: supine, P2: standing, P3: sitting, P4: side lying, P5: cervical flexion supine, P6: cervical extension supine.

Table 3
Results of average peak to peak interval time in 6 postures with CBS (unit: second).

Subject No.	P1	P2	P3	P4	P5	P6
Subject 1	5.27 ± 1.62	4.81 ± 0.69	4.48 ± 1.87	3.13 ± 0.59	5.22 ± 1.49	6.74 ± 1.21
Subject 2	6.34 ± 0.72	4.92 ± 0.77	5.61 ± 0.90	5.13 ± 1.07	6.64 ± 0.83	7.11 ± 0.94
Subject 3	4.87 ± 0.88	4.10 ± 0.51	4.18 ± 0.40	4.5 ± 0.66	4.54 ± 0.55	5.03 ± 0.68
Subject 4	4.72 ± 0.35	3.81 ± 0.25	4.04 ± 0.36	4.64 ± 0.39	5.10 ± 0.58	4.70 ± 0.42
Subject 5	9.13 ± 2.40	7.29 ± 0.70	8.74 ± 1.13	5.41 ± 0.62	6.54 ± 1.93	12.68 ± 1.60
Subject 6	3.61 ± 0.52	2.64 ± 0.40	2.54 ± 0.42	3.28 ± 0.35	3.74 ± 0.39	4.50 ± 0.81
Subject 7	10.42 ± 1.56	4.67 ± 0.90	5.95 ± 0.86	5.93 ± 1.15	8.77 ± 2.40	7.63 ± 1.40
AVG	6.33	4.60	5.07	4.57	5.79	6.91
SD	2.51	1.42	1.96	1.05	1.66	2.83

P1: supine, P2: standing, P3: sitting, P4: side lying, P5: cervical flexion supine, P6: cervical extension supine.

Table 4
Results of average peak to peak interval time in 6 postures with MP150 (unit: second).

Subject No.	P1	P2	P3	P4	P5	P6
Subject 1	5.30 ± 1.59	4.81 ± 0.74	4.50 ± 1.82	3.12 ± 0.55	5.16 ± 1.33	6.67 ± 1.18
Subject 2	6.44 ± 0.86	4.87 ± 0.71	5.54 ± 0.64	5.13 ± 0.86	6.63 ± 0.92	7.25 ± 0.89
Subject 3	4.87 ± 0.81	4.10 ± 0.44	4.17 ± 0.33	4.50 ± 0.61	4.54 ± 0.51	4.97 ± 0.60
Subject 4	4.72 ± 0.64	3.82 ± 0.49	3.99 ± 0.46	4.63 ± 0.32	5.14 ± 0.66	4.70 ± 0.48
Subject 5	9.27 ± 2.62	7.32 ± 0.85	8.72 ± 0.86	5.43 ± 0.59	6.56 ± 1.81	12.67 ± 1.72
Subject 6	3.63 ± 0.23	2.64 ± 0.33	2.54 ± 0.35	3.29 ± 0.22	3.75 ± 0.30	4.51 ± 0.68
Subject 7	10.10 ± 0.91	4.66 ± 0.57	5.98 ± 0.66	5.98 ± 1.08	8.59 ± 1.92	7.56 ± 1.18
AVG	6.33	4.60	5.06	4.58	5.76	6.90
SD	2.44	1.42	1.96	1.06	1.61	2.83

P1: supine, P2: standing, P3: sitting, P4: side lying, P5: cervical flexion supine, P6: cervical extension supine.

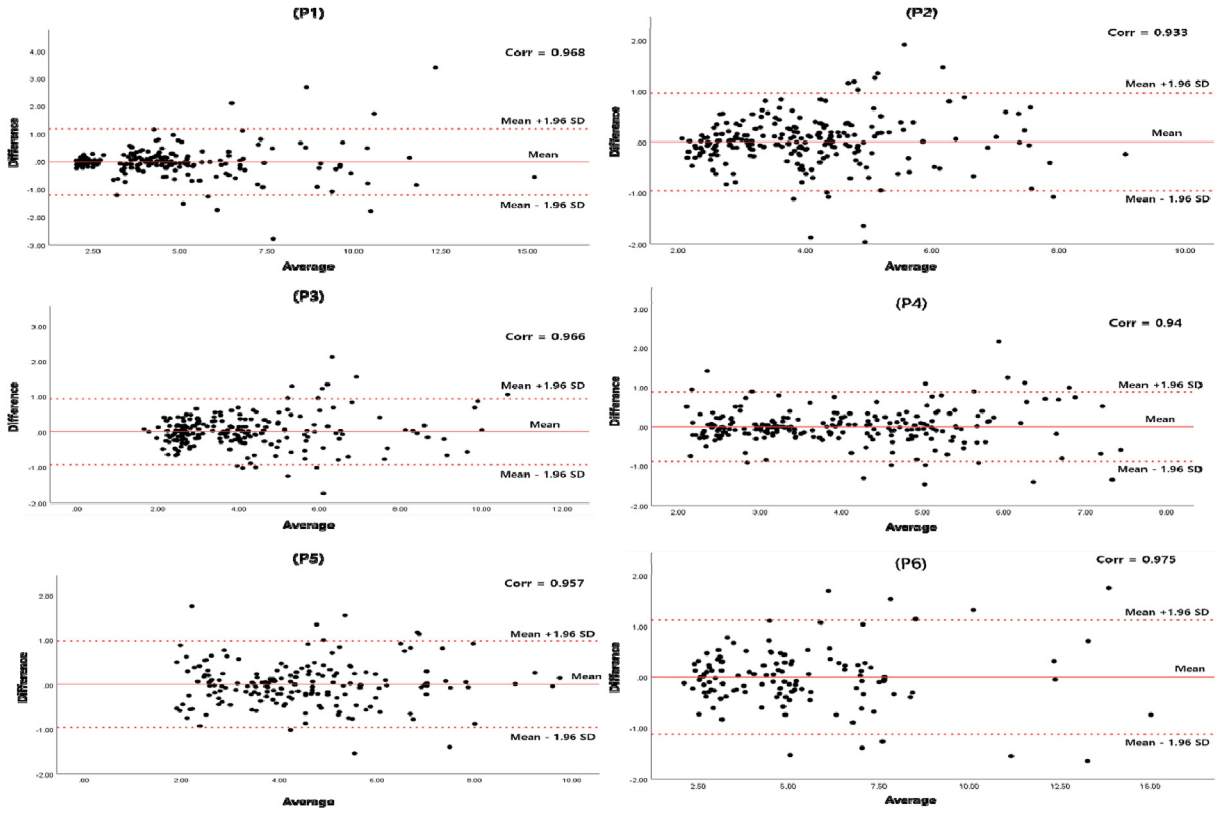

Fig. 7. Bland-Altman plot showing the difference of peak to peak interval time of all subjects in each posture between CBS and MP150. The solid line indicates the mean value of the difference and the dotted lines above and below denote standard deviation (95% CI).

Table 5
Correlation analysis result of peak to peak interval time between CBS and MP150.

Subject No.	Value	P1	P2	P3	P4	P5	P6
Subject 1	R^2	0.95**	0.92**	0.94**	0.95**	0.95**	0.89**
	p-value	0.00	0.00	0.00	0.00	0.00	0.00
Subject 2	R^2	0.87**	0.87**	0.95**	0.89**	0.92**	0.85**
	p-value	0.00	0.00	0.00	0.00	0.00	0.00
Subject 3	R^2	0.97**	0.91**	0.85**	0.96**	0.92**	0.92**
	p-value	0.00	0.00	0.00	0.00	0.00	0.00
Subject 4	R^2	0.80**	0.87**	0.89**	0.93**	0.82**	0.87**
	p-value	0.00	0.00	0.00	0.00	0.00	0.00
Subject 5	R^2	0.96**	0.97**	0.96**	0.95**	0.98**	0.94*
	p-value	0.00	0.00	0.00	0.00	0.00	0.03
Subject 6	R^2	0.96**	0.87**	0.87**	0.89**	0.87**	0.94**
	p-value	0.00	0.00	0.00	0.00	0.00	0.00
Subject 7	R^2	0.90**	0.96**	0.91**	0.91**	0.94**	0.88**
	p-value	0.00	0.00	0.00	0.00	0.01	0.00
AVG	R^2	0.91	0.90	0.90	0.92	0.91	0.89

P1: supine, P2: standing, P3: sitting, P4: side lying, P5: cervical flexion supine, P6: cervical extension supine.
Significance level: **P-value < 0.01, *P-value < 0.05.

respectively, showing a very high correlation ($p \leq 0.05$).

3.1.3. Respiratory rate (RR)

As presented in Table 6, the results of average RR detected by CBS in 6 postures were 10.46 ± 3.81 (P1), 13.84 ± 4.54 (P2), 13.31 ± 5.46 (P3), 13.60 ± 3.59 (P4), 11.56 ± 2.82 (P5), and 10.12 ± 3.13 (P6), respectively. Average RRs detected by MP150 were 10.41 ± 3.71 (P1), 13.82 ± 4.50 (P2), 13.28 ± 5.44 (P3), 13.51 ± 3.62 (P4), 11.49 ± 2.83 (P5), and 10.16 ± 3.11 (P6), respectively (Table 6). In both sensors, the highest RR was found in standing (P2) and the lowest in supine with the neck extended (P6). Fig. 8 shows the result of correlation analysis on RR between the two sensors ($R^2 = 0.99$, p-value $= 0.00$).

Table 6
Results of average respiratory rate detected by CBS and MP150.

Subject No.	P1 (CBS/ MP150)	P2 (CBS/ MP150)	P3 (CBS/ MP150)	P4 (CBS/ MP150)	P5 (CBS/ MP150)	P6 (CBS/ MP150)
Subject 1	11.61/11.55	12.19/12.23	14.38/14.26	19.28/19.28	12.90/13.07	10.83/11.01
Subject 2	9.08/8.99	11.99/12.03	10.44/10.44	11.70/11.52	11.86/11.54	11.05/11.05
Subject 3	12.10/12.06	14.32/14.26	13.95/13.92	13.08/13.02	12.84/12.84	11.56/11.66
Subject 4	12.27/12.42	15.28/15.44	14.45/14.70	12.51/12.50	11.38/11.34	12.35/12.38
Subject 5	6.42/6.37	7.77/7.77	6.47/6.45	10.71/10.63	9.53/9.35	4.27/4.28
Subject 6	16.40/16.05	22.63/22.47	23.74/23.60	17.95/17.81	15.69/15.54	13.23/13.10
Subject 7	5.33/5.43	12.74/12.52	9.77/9.62	9.99/9.80	6.75/6.72	7.57/7.61
AVG	10.46/10.41	13.84/13.82	13.31/13.28	13.60/13.51	11.56/11.49	10.12/10.16
SD	3.81/3.71	4.54/4.50	5.46/5.44	3.59/3.62	2.82/2.83	3.13/3.11

P1: supine, P2: standing, P3: sitting, P4: side lying, P5: cervical flexion supine, P6: cervical extension supine.

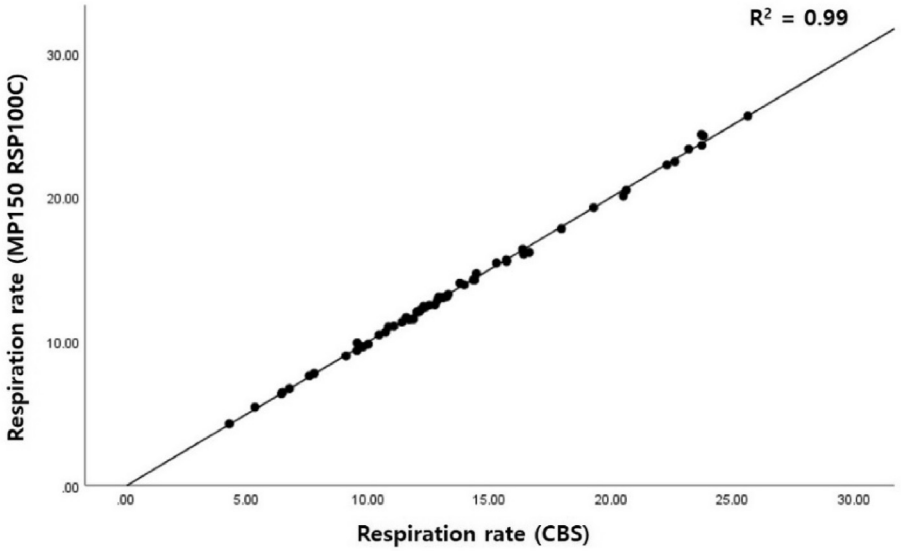

Fig. 8. The result of correlation analysis on respiratory rate between CBS and MP150.

3.2. Results of posture-dependent respiration pattern change detection

3.2.1. Morphological difference captured by CBS and MP150

The raw signal data of RR collected by CBS and MP150 in each of the six postural conditions are shown in Fig. 9. Both the two sensors were able to detect the difference and changes of RR as the subjects changed their postures. Probability analysis was performed to calculate the sensors' capability of detecting a certain posture based on RR signal (Schulz, Bär, & Voss, 2015). The results showed that CBS was able to differentiate P1 from other postures for 85%, P2 for 82%, P3 for 77%, P4 for 82%, P5 for 74%, and P6 for 82%. The detection rates of MP150 were 88%, 82%, 77%, 82%, 74%, and 85%, respectively.

3.2.2. Summarized respiratory pattern difference in each posture

All the three respiratory parameters (RC, PPI, RR) showed to be noticeably changing in different postures. Fig. 10 visualizes the changes detected by CBS and the analyzed results under 6 different postural conditions in this study. For CBS, the average RCs were 20.86 ± 7.49 (P1), 27.57 ± 8.98 (P2), 26.14 ± 10.62 (P3), 27 ± 6.93 (P4), 21.43 ± 5.71 (P5), and 18.71 ± 6.29 (P6); the average PPIs were 6.33 ± 2.51 (P1), 4.60 ± 1.42 (P2), 5.07 ± 1.96 (P3), 4.57 ± 1.05 (P4), 5.79 ± 1.66 (P5), and 6.91 ± 2.83 (P6); the average RRs were 10.46 ± 3.81 (P1), 13.84 ± 4.54 (P2), 13.31 ± 5.46 (P3), 13.60 ± 3.59 (P4), 11.56 ± 2.82 (P5), and 10.12 ± 3.13 (P6).

The patterns of RC and RR were similar as they were both referring to the number of breaths taken within a given time; 2 min and 1 min, respectively. The highest RR was detected in standing posture (P2). This could mean that standing is relatively the most energy-consuming, difficult, and uncomfortable posture among the six postures and thus it increases respiration rate. On the other hand, the lowest RR was in cervical extension supine (P6), underpinning the theory that cervical extension opens up the airway, making inhalation easier in a relaxed pattern. RRs detected in side lying and sitting were found to be different but not as significant. RR was noticeably different between sitting and cervical flexion supine. Breathing with the neck flexed reduces the air intake because it narrows the airway. Thus, sitting posture with neutral head position had significantly higher RR compared to that of cervical flexion supine.

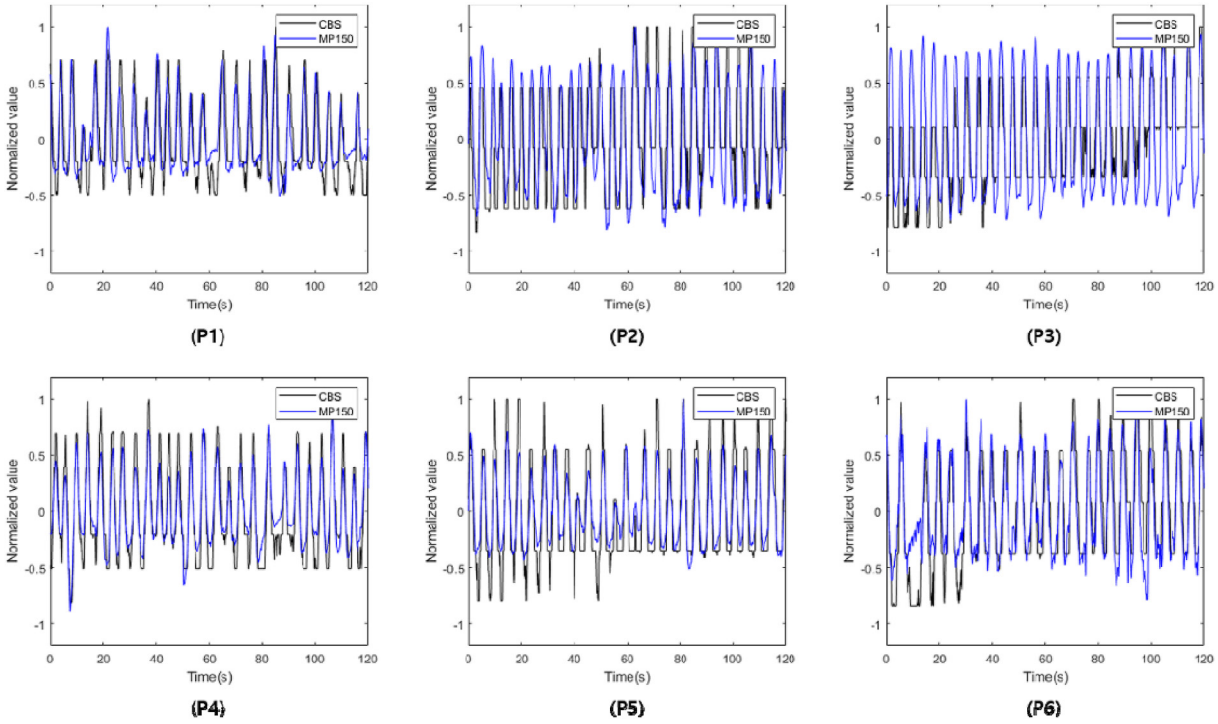

Fig. 9. Morphological overlay comparison of moving average filtered respiratory rate raw data between CBS and MP150 (subject 3). (P1: supine, P2: standing, P3: sitting, P4: side lying, P5: cervical flexion supine, P6: cervical extension supine).

The summarized result shown in Fig. 10 was drawn based on within-subject comparison results, considering individual characteristics and difference in respiration pattern. Summed average values of all 7 subjects were used for analysis.

3.2.3. Error rate of CBS

The error rate of CBS was examined using RR values from each posture. The average error rate was 1.14 ± 0.70 (P1), 0.67 ± 0.57 (P2), 0.74 ± 0.65 (P3), 0.79 ± 0.71 (P4), 1.08 ± 0.96 (P5), and 0.70 ± 0.55 (P6), respectively (Table 7). The error rate of the proposed sensor was less than 2% for each posture.

4. Discussion

In this paper, an advanced version of our first-generation analog circuit-based capacitive textile belt sensor (Min et al., 2014) was studied. With the aim to find solutions for real-life breathing pattern monitoring with a comfortable and practical sensor, an easy-wear CBS was developed with smaller hardware, higher resolution, and wireless function. Its accuracy and feasibility for detecting respiration changes in 6 representative postures in daily living were conducted and three respiration parameters (RC, PPI, RR) were compared between CBS and MP150.

The performance and accuracy of our proposed sensor were confirmed; the results of correlation analysis between the two sensors showed a very high agreement, showing 89 to 100 percent consistency in all three of the respiratory parameters (RC: 100%, PPI: $R^2 \geq 0.89$, RR: $R^2 \geq 0.99$) analyzed in this paper. Although our previous study examined and confirmed the precision of our first generation capacitive textile belt sensor for respiration monitoring (Min et al., 2014), the study was conducted in sitting posture and the belt was worn on the abdomen (navel area). Therefore, the present study aimed to examine the reproducibility of our sensor under various yet more natural postures considering regular daily activities and on a different sensor placement (T4) to detect the circumference changes caused by chest expansions during respirations at rest. Results of this study validated the suitability of T4 for belt-type sensor location area to monitor daily respiration.

The highest RC during 2 min of breathing was found in standing (27.57 ± 8.98), then in the decreasing order: side lying (27 ± 6.93), sitting (26.14 ± 10.62), cervical flexion supine (21.43 ± 5.71), neutral supine (20.86 ± 7.49), and cervical extension supine (18.71 ± 6.29). These results agreed with that of Guan et al.'s study with healthy adults where the highest breathing rate was monitored in standing posture (20 bpm), then in sitting (18 bpm), and the lowest in supine position (15 bpm) (Guan et al., 2018; Hwangbo, Lee, Park, & Han, 2017). RCs in three other postures (side lying, cervical flexion supine, and extension supine) were not comparable because they were not tested in other studies.

The results of PPI values in descending numerical order were cervical extension supine posture (6.91 ± 2.83), neutral supine (6.33 ± 2.51), in cervical flexion supine (5.79 ± 1.66), in sitting (5.07 ± 1.96), in standing (4.60 ± 1.42), and in side lying (4.57 ± 1.05).

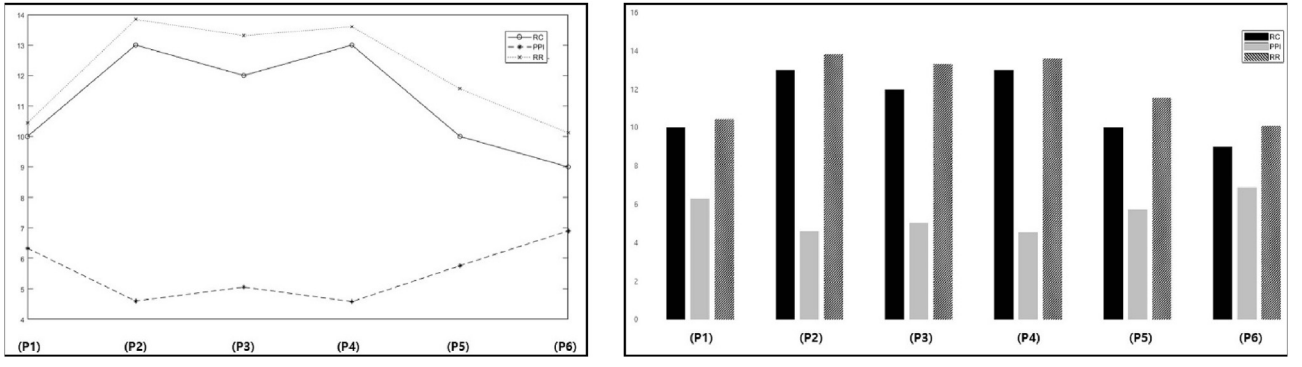

Fig. 10. Summarized CBS detection result in line and bar graph showing the pattern of three respiratory parameters changing according to postures (P1: supine, P2: standing, P3: sitting, P4: side lying, P5: cervical flexion supine, P6: cervical extension supine) (RC: total respiratory count (number), PPI: peak to peak interval time (seconds), RR: respiratory rate (seconds)).

Table 7
Error rate of respiratory rate detected by CBS in 6 conditional postures (%).

Subject No.	P1	P2	P3	P4	P5	P6
Subject 1	0.54	0.35	0.80	0.01	1.29	1.72
Subject 2	1.07	0.38	0.02	1.54	2.76	0.08
Subject 3	0.31	0.43	0.23	0.45	0.02	0.89
Subject 4	1.18	1.03	1.68	0.13	0.39	0.24
Subject 5	0.74	0.03	0.32	0.73	1.85	0.42
Subject 6	2.16	0.72	0.57	0.74	0.92	0.98
Subject 7	1.97	1.76	1.57	1.93	0.35	0.55
AVG	1.14	0.67	0.74	0.79	1.08	0.70
SD	0.70	0.57	0.65	0.71	0.96	0.55

P1: supine, P2: standing, P3: sitting, P4: side lying, P5: cervical flexion supine, P6: cervical extension supine.

The highest PPI was found in supine with the neck extended (P6) and the lowest in side-lying (P4), showing that respiration slowed down in P6 posture. Normally, RC and PPI patterns are inversely related, because higher number of RC naturally causes decreased PPI time. However, there were few outliers in the results (Fig. 7). These may have been due to different physical characteristics and breathing patterns of each subject. The subject inclusion criteria for this study did not take account of the lifestyles of participants such as the amount of their daily physical exercise, smoking, eating, sleeping, and etc. Another factor that may have caused the outliers could be personal preference of certain body postures. For example, side-lying postures can be preferred over supine depending on a person's preferred sleeping postures or just from a habitual posture, which makes the person feel more comfortable in. Comfortable postures can make a person's breathing rate slow down and these postures may be different for every individual.

RR is the frequency of breaths taken within a certain amount of time, usually within 1 min (Krehel et al., 2014). Thus, the results of RR were similar to those of RC. RR is known to have high correlation with gas composition in the blood. Normal range of healthy adult RR is between 12 and 18 breaths per minute at rest. Faster breathing can occur when blood oxygen level is low, and any abnormality in RR can mirror ventilation malfunctions. The results of RR in this study showed to have exactly the same pattern with RC; the highest rate was during standing (13.84 ± 4.54), then in the decreasing order: side lying (13.60 ± 3.59), sitting (13.31 ± 5.46), cervical flexion supine (11.56 ± 2.82), neutral supine (10.46 ± 3.81), and cervical extension supine (10.12 ± 3.13). These results underpin the previous findings which stated that supine position increases blood flow in the pulmonary circulation and consequently decreases the volume of gas inhaled into the thoracic cavity, reducing inhalation (Hwangbo et al., 2017). As all six postures were kept static throughout the experiment, the RRs detected by our sensor were within the normal range, confirming the performance and feasibility of our sensor.

This means that standing is relatively the most energy-consuming, difficult, and uncomfortable posture affecting respiration rate to increase. Subjects were breathing more frequently within the observed time range during standing. This agrees with the results of the previous studies that reported oxygen uptake decreased the most in standing or trunk forward leaning, then in sitting, and lastly in supine posture, meaning that the highest oxygen uptake was observed in the supine posture (Hwangbo et al., 2017). In the present study, supine posture was divided into three neck positions to examine the differences considering people's resting or sleeping postures. The results showed that supine posture with cervical extension of 45° seemed to be the most effective way to breathe. Moreover, supine with cervical flexion of 45° had the highest RR and RC among the 3 different supine postures. Various types of supine postures especially with different neck postures are directly related to sleep apnea and hypopnea due to airway obstruction (Lee et al., 2018). As our sensor was able to detect these differences, potential application in sleep apnea monitoring, respiratory disease prevention, and early detection of diagnostic symptoms has been confirmed.

A limitation of this study was small sample number and gender-oriented design, making it inappropriate to generalize the results. However, the results may still have significance in laying the foundation for possibility to utilize and extend the application of capacitance belt sensor to detect and monitor posture-dependent respiration changes. Initially, we intended to compare 8 postures including prone and right side-lying postures. However, neither of the two sensors (CBS and MP150) used in this study were able to detect stable breathing signals in prone and right side lying for analysis. This may be due to the sensors' location and mechanism of signal detection; both sensors were placed on the chest (2 cm laterally distanced from xyphoid process, on pectoralis major muscle) and breathing pattern was detected according to the resistance against the sensor caused by chest circumference expansion and diminution during respiration.

In our future studies, we plan to add a sensor on the back of the trunk to monitor respiration changes in prone and also during dynamic daily activities. We will try finding the optimum sensor placement area by comparing sensor performance in various locations of the human body. Studies on subjects with a wider range of age and patients with diverse pulmonary symptoms are also needed.

5. Conclusion

The newly developed wearable capacitive belt sensor was confirmed to have similar functions and accuracy to those of a reputational commercial sensor in detecting respiration count, peak to peak interval, and respiratory rate during respiration at rest in 6 different postures that are considered representative of daily activities. It is feasible to apply the proposed sensor for detecting and analyzing the changes in posture-dependent respiration.

Acknowledgments

This research was supported by Basic Science Research Program through the National Research Foundation of Korea (NRF) funded by the Ministry of Education (NRF-2018R1D1A1B07050037).

This research was supported by the Bio & Medical Technology Development Program of the National Research Foundation (NRF) funded by the Ministry of Science, ICT & Future Planning (NRF-2015M3A9D7067388).

References

Al-Khalidi, F. Q., Saatchi, R., Burke, D., Elphick, H., & Tan, S. (2011). Respiration rate monitoring methods: A review. *Pediatric Pulmonology, 46*(6), 523–529. https://doi.org/10.1002/ppul.21416.

Aliverti, A., Dellaca, R., Pelosi, P., Chiumello, D., Gatihnoni, L., & Pedoti, A. (2001). Compartmental analysis of breathing in the supine and prone positions by optoelectronic plethysmography. *Annals of Biomedical Engineering, 29*(1), 60–70.

Cesareo, A., Previtali, Y., Biffi, E., & Aliverti, A. (2018). Assessment of breathing parameters using an inertial measurement unit (IMU)-Based system. *Sensors (Basel), 19*(1). https://doi.org/10.3390/s19010088.

Chhabra, S. K. (2015). Interpretation of spirometry: Selection of predicted values and defining abnormality. *Indian Journal of Chest Diseases and Allied Sciences, 57*(2), 91–105.

Fekr, A. R., Radecka, K., & Zilic, Z. (2015). Design and evaluation of an intelligent remote tidal volume variability monitoring system in E-health applications. *IEEE Journal Biomedical Health Inform, 19*(5), 1532–1548. https://doi.org/10.1109/JBHI.2015.2445783.

Guan, H., Yang, X., Sun, W., Ren, A., Fan, D., Zhao, N., et al. (2018). Posture-specific breathing detection. *Sensors (Basel), 18*(12). https://doi.org/10.3390/s18124443.

Houssein, A., Ge, D., Gastinger, S., Dumond, R., & Prioux, J. (2019). Estimation of respiratory variables from thoracoabdominal breathing distance: A review of different techniques and calibration methods. *Physiological Measurement.* https://doi.org/10.1088/1361-6579/ab0b63.

Hughes, J., & Iida, F. (2018). Multi-functional soft strain sensors for wearable physiological monitoring. *Sensors (Basel), 18*(11). https://doi.org/10.3390/s18113822.

Hwangbo, G., Lee, D. H., Park, S. H., & Han, J. W. (2017). Changes in cardiopulmonary function according to posture during recovery after maximal exercise. *Journal of Physical Therapy Science, 29*(7), 1163–1166. https://doi.org/10.1589/jpts.29.1163.

Krehel, M., Schmid, M., Rossi, R. M., Boesel, L. F., Bona, G. L., & Scherer, L. J. (2014). An optical fibre-based sensor for respiratory monitoring. *Sensors (Basel), 14*(7), 13088–13101. https://doi.org/10.3390/s140713088.

Lee, M. H., Jang, G. Y., Kim, Y. E., Yoo, P. J., Wi, H., Oh, T. I., et al. (2018). Portable multi-parameter electrical impedance tomography for sleep apnea and hypoventilation monitoring: Feasibility study. *Physiological Measurement, 39*(12), 124004. https://doi.org/10.1088/1361-6579/aaf271.

Li, R., Nie, B., Zhai, C., Cao, J., Pan, J., Chi, Y. W., et al. (2016). Telemedical wearable sensing platform for management of chronic venous disorder. *Annals of Biomedical Engineering, 44*(7), 2282–2291. https://doi.org/10.1007/s10439-015-1498-x.

Min, S. D., Yun, Y., & Shin, H. (2014). Simplified structural textile respiration sensor based on capacitive pressure sensing method. *IEEE Sensors Journal, 14*(9), 3245–3251.

Nie, Z., Nijhuis, C. A., Gong, J., Chen, X., Kumachev, A., Martinez, A. W., et al. (2010). Electrochemical sensing in paper-based microfluidic devices. *Lab on a Chip, 10*(4), 477–483. https://doi.org/10.1039/b917150a.

Nozoe, M., Mase, K., Takashima, S., Matsushita, K., Kouyama, Y., Hashizume, H., et al. (2014). Measurements of chest wall volume variation during tidal breathing in the supine and lateral positions in healthy subjects. *Respiratory Physiology & Neurobiology, 193*, 38–42. https://doi.org/10.1016/j.resp.2013.12.016.

Pegan, J. D., Zhang, J., Chu, M., Nguyen, T., Park, S. J., Paul, A., et al. (2016). Skin-mountable stretch sensor for wearable health monitoring. *Nanoscale, 8*(39), 17295–17303. https://doi.org/10.1039/c6nr04467k.

Reyes, B. A., Reljin, N., Kong, Y., Nam, Y., & Chon, K. H. (2017). Tidal volume and instantaneous respiration rate estimation using a volumetric surrogate signal acquired via a smartphone camera. *IEEE Journal Biomedical Health Inform, 21*(3), 764–777. https://doi.org/10.1109/JBHI.2016.2532876.

Romei, M., Mauro, A. L., D'Angelo, M. G., Turconi, A. C., Bresolin, N., Pedotti, A., et al. (2010). Effects of gender and posture on thoraco-abdominal kinematics during quiet breathing in healthy adults. *Respiratory Physiology & Neurobiology, 172*(3), 184–191. https://doi.org/10.1016/j.resp.2010.05.018.

Schellongowski, P., Losert, H., Locker, G. J., Laczika, K., Frass, M., Holzinger, U., et al. (2007). Prolonged lateral steep position impairs respiratory mechanics during continuous lateral rotation therapy in respiratory failure. *Intensive Care Medicine, 33*(4), 625–631. https://doi.org/10.1007/s00134-006-0513-y.

Schlesinger, J. J. (2015). Applications of a noninvasive respiratory volume monitor for critical care medicine. *Respiratory Care, 60*(5), e97–100. https://doi.org/10.4187/respcare.03744.

Schulz, S., Bär, K., & Voss, A. (2015). Analyses of heart rate, respiration and cardiorespiratory coupling in patients with schizophrenia. *MDPI Entropy, 17*(2), 483–501. https://doi.org/10.3390/e17020483.

Sukul, P., Trefz, P., Kamysek, S., Schubert, J. K., & Miekisch, W. (2015). Instant effects of changing body positions on compositions of exhaled breath. *Journal of Breath Research, 9*(4), 047105. https://doi.org/10.1088/1752-7155/9/4/047105.

Terazawa, M., Karita, M., Kumagai, S., & Sasaki, M. (2018). Respiratory motion sensor measuring capacitance constructed across skin in daily activities. *Micromachines (Basel), 9*(11). https://doi.org/10.3390/mi9110543.

Yang, J., Keller, J. M., Popescu, M., & Skubic, M. (2016). Sleep stage recognition using respiration signal. In *2016 38th annual international conference of the IEEE engineering in medicine and biology society* (pp. 2843–2846). EMBC.

Zens, M., Niemeyer, P., Bernstein, A., Feucht, M. J., Kuhle, J., Sudkamp, N. P., et al. (2015). Novel approach to dynamic knee laxity measurement using capacitive strain gauges. *Knee Surgery, Sports Traumatology, Arthroscopy, 23*(10), 2868–2875. https://doi.org/10.1007/s00167-015-3771-9.